Prevalence of the sling effect for enhancing collision rates in turbulent suspensions

Michel Voßkuhle[1]**, Alain Pumir**[1,2,†]**, Emmanuel Lévêque**[3] **and Michael Wilkinson**[4]

[1]Laboratoire de Physique, Ecole Normale Supérieure de Lyon, CNRS, Université de Lyon, 69007 Lyon, France

[2]Max-Planck Institute for Dynamics and Self-Organisation, 37077 Göttingen, Germany

[3]Laboratoire de Mécanique des Fluides et d'Acoustique, Ecole Centrale de Lyon, CNRS, Université de Lyon, 69134 Ecully CEDEX, France

[4]Department of Mathematics and Statistics, The Open University, Walton Hall, Milton Keynes MK7 6AA, UK

Turbulence facilitates collisions between particles suspended in a turbulent flow. Two effects have been proposed that can enhance the collision rate at high turbulence intensities: 'preferential concentration' (a clustering phenomenon) and the 'sling effect' (arising from the formation of caustic folds in the phase space of the suspended particles). We have determined numerically the collision rate of small heavy particles as a function of their size and densities. The dependence on particle densities allows us to quantify the contribution of the sling effect to the collision rate. Our results demonstrate that the sling effect provides the dominant mechanism to the enhancement of the collision rate of particles, when inertia becomes significant.

---

1. Introduction

Understanding the rate of collisions between small particles, suspended in a turbulent fluid, is necessary for describing a variety of important physical processes. In the case of clouds, collisions between droplets may determine the onset of rainfall (Shaw 2003). Models for planet formation involve aggregation through collisions of dust grains in the circumstellar disc (Safranov 1969). Also, collisions between suspended particles may be an important contribution to dissipation of energy in some particle-laden flows (Elghobashi 1994). It is, therefore, of considerable importance to quantify collisions between particles suspended in a turbulent gas.

This topic has a long history (recently reviewed by Grabowski & Wang 2013), starting from the seminal work by Saffman & Turner (1956), who were interested in understanding rain initiation in turbulent clouds. Important theoretical insights have emerged in recent years, which indicate that their results lead to an underprediction of the collision rate in highly turbulent flows. Saffman & Turner remarked that,

† Email address for correspondence: alain.pumir@ens-lyon.fr

because of the inertia of the suspended particles, there is a differential acceleration between the fluid and the particles. Two mechanisms whereby this inertial effect can influence the collision rate have been identified. First, inertia is responsible for a strong clustering of particles, an effect termed 'preferential concentration', which is ascribed to (heavy) particles being expelled from vortices by a centrifugal effect (Maxey 1987) (other interpretations are considered by Wilkinson *et al.* (2007)). This clustering effect enhances the local concentration, hence the collision rate. Secondly, owing to inertia, the relative velocity between two particles can be enhanced. It has been realised recently that this mechanism may lead to particles being arbitrarily close, and yet having very different velocities. This induces collisions that may be thought as resulting from particles being 'slung' by vortices (Falkovich, Fouxon & Stepanov 2002). This phenomenon can also be understood in terms of caustics in the phase space of the suspended particles (Wilkinson & Mehlig 2005; Wilkinson, Mehlig & Bezuglyy 2006), and has recently been demonstrated experimentally (Bewley, Saw & Bodenschatz 2013). When the turbulence is sufficiently intense, a gas-kinetic model can be used to describe the trajectories (Abrahamson 1975), sometimes referred to as 'random uncorrelated motion' (IJzermans, Meneguz & Reeks 2010; Meneguz & Reeks 2011).

These mechanisms for enhancement of the collision rate have been illustrated by simulations on model flows (Ducasse & Pumir 2009; Meneguz & Reeks 2011). There have been investigations of the collision rates in simulations of fully developed turbulence, which have provided quantitative information on preferential concentration and on the increase of the collision velocity (Sundaram & Collins 1997; Wang, Wexler & Zhou 2000; Rosa *et al.* 2013). There have also been detailed theoretical investigations of the collision rate: a particularly effective description of the collision-rate enhancement in terms of a stochastic model for the probability distribution function (p.d.f.) of pairs of particles has been proposed by Zaichik, Simonin & Alipchenkov (2003). These approaches do not make any attempt at separating the contributions from the two different mechanisms of collision-rate enhancement. In this paper we report direct numerical simulation (DNS) studies of the collision rate of particles in fully developed three-dimensional turbulence, as a function of both their size and density. This extended parameter space allows us to separate the clustering and the caustics/sling effect. We find that the caustics/sling effect plays a significant role in the mechanism leading to the enhanced collision rate in turbulent flows when the response time of the particle exceeds the Kolmogorov time scale of the flow ($St \geqslant 1$, with the definition (2.3) below).

2. Models for the collision rate

In this section we discuss the clustering and sling/caustics models for the collision rate, before considering how these compare with our numerical results. We consider a monodisperse suspension of spherical particles, of radius a, made of material with density ρ_p, suspended in an incompressible fluid of density ρ_f and kinematic viscosity ν. The fluid, with velocity field $\boldsymbol{u}(\boldsymbol{r}, t)$, is in a statistically steady state of turbulent motion with rate of dissipation per unit mass equal to ϵ. We consider a sufficiently dilute suspension, so the flow is not significantly perturbed by the presence of the particles. We assume that the particles obey the simple equation of motion (Gatignol 1983; Maxey & Riley 1983)

$$\dot{\boldsymbol{r}} = \boldsymbol{v}, \quad \dot{\boldsymbol{v}} = \frac{1}{\tau_p}[\boldsymbol{u}(\boldsymbol{r}, t) - \boldsymbol{v}], \quad (2.1a,b)$$

where

$$\tau_p = \frac{2}{9} \frac{a^2}{\nu} \frac{\rho_p}{\rho_f} \tag{2.2}$$

is the particle relaxation time, determined from Stokes formula for the drag on a moving sphere. This equation of motion is valid in the limit where the suspended particles are very small and very dense: $\rho_p/\rho_f \gg 1$.

In determining the motion of particles by using (2.1), only one parameter is needed, namely the relaxation time τ_p. To compare this time scale to a time scale of the flow, we introduce the Stokes number, as the ratio between τ_p and the characteristic time of the flow at the smallest scale, the Kolmogorov time scale $\tau_K \equiv (\nu/\epsilon)^{1/2}$:

$$St = \frac{\tau_p}{\tau_K}. \tag{2.3}$$

The Stokes number parametrises the effect of particle inertia. For $St \ll 1$, particles are advected by the fluid, and collisions are the result of shear. When $St \gg 1$, the inertia of the particles allows them to move relative to the surrounding fluid. Note that $St \propto \sqrt{\epsilon}$, so that the inertial effects become more important when the turbulent intensity increases. In the range of droplet size relevant in the cloud microphysics context, $10\ \mu m \lesssim a \lesssim 60\ \mu m$, the Stokes number varies in the range $0.01 \leqslant St \leqslant 2$ (Grabowski & Wang 2013). In other applications, such as planet formation, very large Stokes numbers are relevant (Wilkinson, Mehlig & Uski 2008). Gravitational settling is important for cloud microphysics (Grabowski & Vaillancourt 1999), but not for planet formation.

We count a collision as occurring when the separation of the centres of independently moving particles come within $2a$. The collision rate R, defined as the probability per unit time for a given particle to collide with any of the other particles, is proportional to the volume density of the other particles, n_0, to the cross-sectional area ($\propto a^2$) and to the appropriate average of the relative velocity for colliding particles (Wang *et al.* 2000) denoted by $\langle |w| \rangle$:

$$R = 2\pi n_0 (2a)^2 \langle |w| \rangle, \tag{2.4}$$

where w is defined as $w = \delta \boldsymbol{v} \cdot \delta \boldsymbol{r}/|\delta \boldsymbol{r}|$, $\delta \boldsymbol{r}$ being the distance between the centres of the colliding particles, and $\delta \boldsymbol{v}$ the difference between the velocities of the centres of the particles. The expected total number of collisions in a closed system of volume V is simply obtained by multiplying R by $n_0 V/2$. We note that our definition of the collision rate differs slightly from the one used elsewhere, and generally denoted by Γ (see e.g. Sundaram & Collins 1997). The quantity R used here is simply related to Γ, defined among others in Sundaram & Collins (1997), by $R = n_0 \Gamma$. We neglected the role of gravity, and of hydrodynamic interactions, which may inhibit collisions by trapping a lubricating layer between the particles. We are concerned here with the collision rate for this slightly simplified model. The objective is to describe the collision rate determined from our DNS studies within the framework of a parametrisation based upon recent theoretical insights.

In the limit $St \ll 1$ the collision rate is determined by shearing motion, so that $\langle |w| \rangle \sim 2a/\tau_K$. Saffman & Turner (1956) argued that

$$R_{ST} = \sqrt{\frac{8\pi}{15}} \frac{n_0 (2a)^3}{\tau_K}. \tag{2.5}$$

Their calculation includes all instances in which the separation radius decreases past $2a$. In the case of collisions where particles stick or coalesce on contact, we should only count the first contact collisions. This effect should be accounted for by introducing a factor $f < 1$ in (2.5). These corrections, which are investigated in a separate publication (Voßkuhle *et al.* 2013), are not discussed in this article. We simply set $f = 1$ here.

The enhancement of the collision rate, compared to the prediction of (2.5), is expected to come from the particle trajectories breaking away from the fluid as the Stokes number increases. The effect termed 'preferential concentration' causes clustering of particles with finite values of *St*. The density of particles at a distance r from a given test particle is $n_0 g(r)$, where $g(r)$ is a radial correlation function. The expulsion of heavy particles from vorticity-dominated regions induces only minor differences of the relative velocity difference (Chun *et al.* 2005; Gibert, Xu & Bodenschatz 2012). As a result, the collision rate due to particles being advected into contact by shearing motion is

$$R_{adv} = \sqrt{\frac{8\pi}{15}} \frac{n_0 (2a)^3}{\tau_K} g(2a). \tag{2.6}$$

At a fixed Stokes number, the function $g(r)$ has a power-law dependence upon r: $g(r) \propto r^{-\zeta}$ (Reade & Collins 2000). This reflects the expectation that the suspended particles should sample a fractal measure (Sommerer & Ott 1993; Bec 2003). The exponent is $\zeta = d - D_2$, where d is the spatial dimension and D_2 the correlation dimension (Grassberger & Procaccia 1983). DNS results indicate that, for three-dimensional turbulent flows, $2.3 \leqslant D_2 \leqslant 3$ (Bec *et al.* 2007).

In the limiting case where the turbulence intensity is very high, an alternative approach to understanding the effect of increasing the turbulence intensity was initiated by Abrahamson (1975), who pointed out that a gas-kinetic approach can be used to model the motion of the suspended particles. In this limit the relative velocity due to shearing motion induced by turbulence, which is of the order of a/τ_K (Saffman & Turner 1956), is replaced by a much larger relative velocity that characterises the relative motion of the fluid at different positions. This relative velocity may be parametrised by writing $\langle |w| \rangle \sim u_K F(St, Re)$, where $u_K = (\epsilon \nu)^{1/4}$ is the velocity at the Kolmogorov scale, and F depends on the Stokes number, *St*, and the Reynolds number, *Re*. The collision rate is, therefore,

$$R_{sling} = \frac{n_0 a^2 \eta}{\tau_K} F(St, Re), \tag{2.7}$$

where $\eta = (\nu^3/\epsilon)^{1/4}$ is the Kolmogorov length. The collision rate is the sum of contributions from collisions between particles that lie on the same branch of the phase-space manifold, giving rise to R_{adv}, and collisions between particles on different branches, giving rise to R_{sling}:

$$R = R_{adv} + R_{sling}. \tag{2.8}$$

This decomposition, proposed in earlier works (Wilkinson *et al.* 2006; Ducasse & Pumir 2009; Gustavsson & Mehlig 2011), rests on the assumption that the fraction of particles that give rise to preferential concentration collide with a small relative velocity with respect to the fluid, whereas another fraction, evenly distributed in

the fluid, moves with large relative velocity. The collisions due to these particles are described by the term R_{sling}, with the analytic form in (2.7). When $St \to 0$, the collision rate is well approximated by (2.5), but both terms in (2.8) can contribute to an enhanced collision rate as St increases. The principal question addressed by this paper is to determine which contribution dominates as St increases. While an explicit determination of the quantities entering (2.8) is difficult (Ducasse & Pumir 2009), we study here the collision rate R by varying, at fixed values of Re_λ and St, the size of the particles. In view of (2.2) and (2.3), it amounts to varying the density ratio (ρ_p/ρ_f).

It is possible to consider the asymptotic forms for the function $F(St, Re)$ in (2.7), in the limits of small and large Stokes numbers. In the limit as $St \to 0$, we must have $F(St, Re) \to 0$, so that the limiting case (2.5) is recovered from (2.8). Considerations of model systems (described by Wilkinson *et al.* (2006)) suggest that F has non-analytic behaviour in this limit, such as $F(St, Re) \sim \exp(-C/St)$, for some constant C: this is consistent with numerical results with the Navier–Stokes equations (Falkovich & Pumir 2007). The asymptotic form of the function $F(St, Re)$ at large Stokes numbers has been considered by several authors. Abrahamson's theory is not valid for fully developed turbulence, because it ignores the multiscale structure of the flow. A version that correctly accounts for the multiscale structure of turbulence was proposed by Völk *et al.* (1980), using the Kolmogorov model for the structure of the flow. This theory suggests that $F(St, \infty) \sim St^{1/2}$. A simpler and more general dimensional argument was proposed by Mehlig, Uski & Wilkinson (2007): in the inertial range, the relative velocity can depend only upon ϵ and τ_p, so that dimensional analysis mandates that $\langle |w| \rangle \sim \sqrt{\epsilon \tau_p}$. Substituting for τ_p, we have a rate of collision at high Stokes number that is of the form (2.7) with $F(St, \infty) \sim K\sqrt{St}$, where K is a universal dimensionless constant. We emphasise that, because the preferential concentration effect is a consequence of nearby particles experiencing a correlated strain rate, this effect makes no contribution to R_{sling}. Equation (2.7) accounts for collisions between particles that have not experienced the same local environment, and the factor $g(2a)$ that occurs in (2.6) is therefore absent from (2.7).

An alternative approach to the theoretical analysis of collision rates was pursued by Zaichik *et al.* (2003), who analysed the p.d.f. of relative position and velocity in a stochastic model for the turbulent velocity field. This model includes both preferential concentration and the sling/caustic effects, but does not allow their relative contributions to be determined. The possible connections between that approach and the one discussed in this paper deserves further attention (Salazar & Collins 2012).

3. DNS studies of the collision rate

As explained before, we investigated the collision rate R as a function of both a and ρ_p/ρ_f. This allows us, in particular, to keep the values of Re_λ and St fixed, while varying the size of the particles.

Our simulations used a pseudo-spectral code, fully dealiased, with grid size 384^3. The flow is forced with a prescribed energy injection rate ϵ (Lamorgese, Caughey & Pope 2005). The Taylor microscale Reynolds number achieved in the steady state is $Re_\lambda = 130$. Proper spatial resolution has been maintained, as can be judged from the product $k_{max}\eta = 2$, where k_{max} is the largest wavenumber faithfully simulated. Particle trajectories were integrated by using the velocity Verlet algorithm (Press *et al.* 2007) and resorting to tricubic interpolation to evaluate the fluid velocity at the position of the particle. We detected collisions by using the algorithm described by Sundaram & Collins (1996). Modifying the ratio ρ_p/ρ_f at fixed value of the Stokes
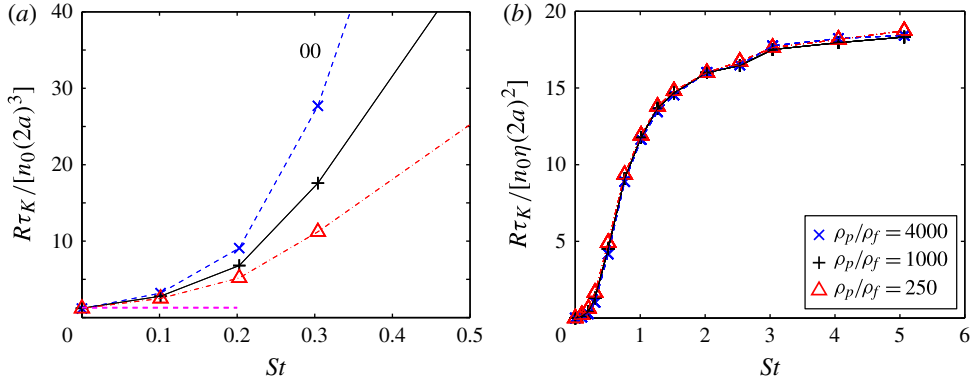
FIGURE 1. (Colour online) The collision rate R as a function of the Stokes number St and for the ratios of density $\rho_p/\rho_f = 250$, 10^3 and 4×10^3. The collision rate R is normalised by (a) $n_0(2a)^3/\tau_K$ and (b) $n_0(2a)^2\eta/\tau_K$. The horizontal dashed line in panel (a) corresponds to the Saffman–Turner prediction. The legend in (b) applies also to (a).

number is achieved by varying in the collision detection algorithm the radius of the particles, a, according to (2.2) and (2.3) (so that $a \propto (\rho_p/\rho_f)^{-1/2}$). In the range of parameters considered, $\rho_p/\rho_f > 250$ and $St \leqslant 5$, the particle radii are at most $\approx \eta/3$, which ensures that (2.1) provides a very good description of the motion. We find that after a transient state of approximately five eddy turnover times, the collision rate becomes independent of time. The collision rates were determined by recording at the minimum 1.3×10^4 collisions when $\rho_p/\rho_f = 10^3$, accumulated (except in one case) over $\gtrsim 10$ eddy turnover times. For the values of St and ρ_p/ρ_f considered here, the particle size a is very small, so the Reynolds number of the particle is negligible, and other corrections to (2.1) can be neglected (Daitche & Tél 2011).

The collision rate, R, determined numerically is plotted in figure 1. As explained earlier, we do not distinguish here between single and multiple collisions. In figure 1(a), R is normalised by $n_0(2a)^3/\tau_K$ and plotted as a function of St. The Saffman–Turner prediction, equation (2.5), implies that, in the limit $St \to 0$, the quantity $R\tau_K/(n_0(2a)^3)$ should become independent of the ratio ρ_p/ρ_f. Our own numerical results are only consistent with this prediction for small values of St. Figure 1(b) shows that $R\tau_K/(n_0 a^2 \eta)$ as a function of the Stokes number does not depend much on ρ_p/ρ_f for values of St larger than $\gtrsim 0.3$. This scaling is consistent with the sling/caustics collision mechanism, described by (2.7). We note that $F(St, Re)$ deduced from figure 1(b) does not fit the asymptotic form $F(St, \infty) = K\sqrt{St}$ for large values of St. We ascribe this to the limited Reynolds number of our numerical simulations.

A clear illustration of the transition from the regime described by the Saffman–Turner prediction, (2.5), to the sling-dominated regime, (2.7), is provided by figure 2, which shows the ratio between the values of R computed at $\rho_p/\rho_f = 4000$ and 1000 (crosses) and $\rho_p/\rho_f = 1000$ and 250 (triangles). Whereas (2.5) predicts that, in the absence of any preferential concentration ($g = 1$), these ratios should be $1/8$, (2.7) rather leads to the expectation of a ratio equal to $1/4$ (recall that $a \propto (\rho_p/\rho_f)^{-1/2}$). The ratio $R_{adv}(4\rho_p/\rho_f)/R_{adv}(\rho_p/\rho_f)$ is equal to $(1/2)^{3-\zeta}$, where ζ characterises the scaling of g as a function of scale. Figure 2 shows that the ratios are extremely close to $1/4$ for $St \gtrsim 0.75$, but approach $1/8$ for $St \lesssim 0.3$. At values of $St \lesssim 0.3$, the comparison
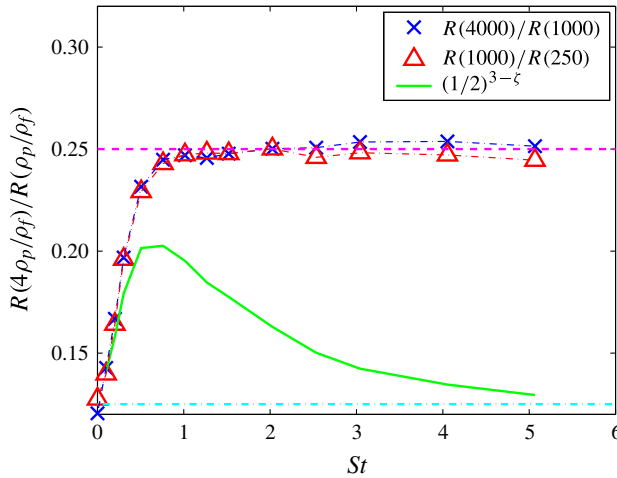
FIGURE 2. (Colour online) The ratio between the two collision rates R corresponding to $\rho_p/\rho_f = 4000$ and 1000 (crosses) and $\rho_p/\rho_f = 1000$ and 250 (triangles), illustrating the crossover between the sling-dominated regime for $St \gtrsim 0.5$, and the regime described by the Saffman–Turner theory for $St \lesssim 0.3$. For the sake of comparison, the continuous line shows the quantity $(1/2)^{3-\zeta}$, which represents the increase of the collision rate R_{adv} due only to the effect of preferential concentration.

of the ratio between the values of R and the values of R_{adv} indicates that preferential concentration is the prevailing mechanism leading to the enhancement of the collision rate. In the intermediate range $0.5 \lesssim St \lesssim 1$, the growing difference between the two ratios of R and R_{adv} points to a transition towards a regime dominated by the sling effect.

Figure 3 shows the function $g(2a)$ (which quantifies the importance of preferential concentration) in our simulations for the three different values of ρ_p/ρ_f. Figure 3 shows that the strong enhancement of the concentration in the vicinity of a particle is not sufficient to make the advective collision rate (2.6) comparable to the sling collision rate, (2.7), as soon as the value of St is larger than $\gtrsim 1$. This conclusion is consistent with the results shown in figure 2.

The observation concerning the ratios between the collision rates at values of $4\rho_p/\rho_f$ and ρ_p/ρ_f shown in figure 2 implies that, provided $St \gtrsim 0.75$, the sling effect becomes very significant. This conclusion is corroborated by figure 4, which shows the value of R_{adv}/R for the values of ρ_p/ρ_f chosen here as a function of St. For the value of $\rho_p/\rho_f = 1000$, relevant to cloud microphysics, the effect due to preferential concentration provides ∼51 % of the total collision rate at $St = 0.75$. This contribution drops to ∼40 % at $St = 1$, and becomes even less significant at higher values of ρ_p/ρ_f. The decrease in the relative contribution of the preferential concentration when ρ_p/ρ_f increases, clearly seen when $St \gtrsim 0.75$ in figure 4, is directly related to the difference between the curves showing $R(4\rho_p/\rho_f)/R(\rho_p/\rho_f)$ and the curve showing $(1/2)^{3-\zeta}$. This difference implies that the relative contribution due to preferential concentration becomes very small when the ratio ρ_p/ρ_f increases, that is, when the particle size diminishes. Thus, in the limit $\rho_p/\rho_f \to \infty$, the sling effect is expected to be the prevailing effect. In the physically very relevant case of water droplets in air, where the ratio ρ_p/ρ_f is large but finite, $(\rho_p/\rho_f = 1000)$, the preferential concentration effect still plays a significant role. Figure 2 shows that the contribution of the preferential
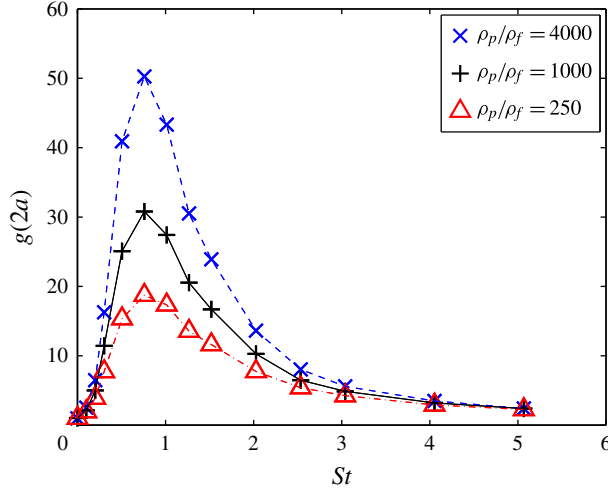
FIGURE 3. (Colour online) The function g that measures preferential concentration, computed for three values of a, corresponding to particles with a density ρ_p equal to $250\rho_f$, $1000\rho_f$ and $4000\rho_f$, as indicated. The preferential concentration does not play a significant role for $St \gtrsim 5$.
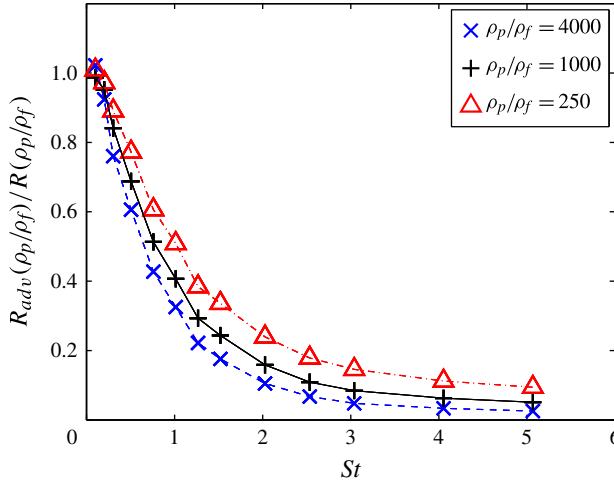

FIGURE 4. (Colour online) The ratio of the contribution to the collision rate due to preferential concentration R_{adv}, defined by (2.6), and of the total collision rate, R. At fixed value of ρ_p/ρ_f, the contribution of R_{adv} to the total collision rate decreases when the Stokes number increases, or when the ratio ρ_p/ρ_f increases.

concentration at $St \approx 0.75$ is $\sim 51\,\%$, and drops to $16\,\%$ at $St = 2$. These values would drop to $43\,\%$ and $10\,\%$ at $\rho_p/\rho_f = 4000$.

Further evidence for the importance of caustics comes from considering the probability density, $P(w|2a)$, of the radial relative velocity between two particles, $w \equiv \delta \boldsymbol{v} \cdot \delta \boldsymbol{r}/|\delta \boldsymbol{r}|$, conditioned on the fact that the two particles collide ($|\delta \boldsymbol{r}| = 2a$ and $w \leqslant 0$). The quantity $P(w|2a)$ was determined from our simulations by first determining the distribution of velocity $P_{coll}(w)$ (for $w \leqslant 0$). As the number of particle pairs
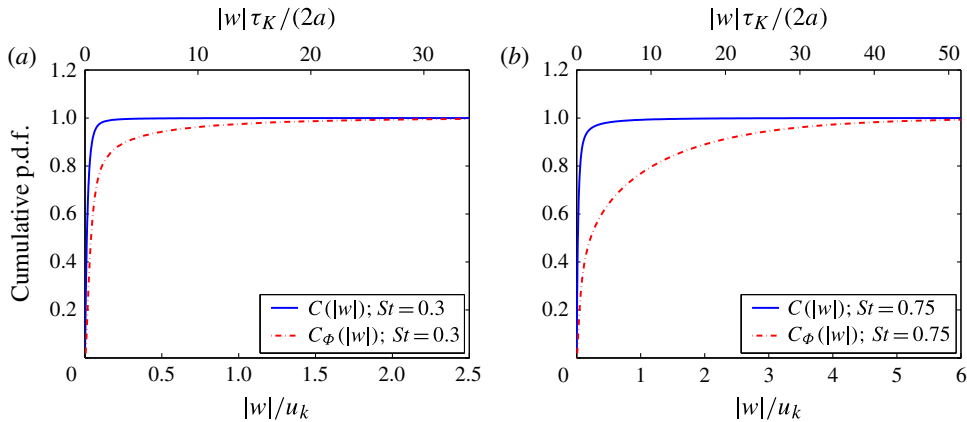
FIGURE 5. (Colour online) The cumulative distribution of radial velocities of colliding particles, $C(|w|)$ (continuous line), and the cumulative distribution weighted by $|w|$, $C_\Phi(|w|)$ (dashed-dotted line), defined by (3.2). These describe, for the two Stokes numbers shown here, (a) $St = 0.3$ and (b) $St = 0.75$, the contribution to the collision rate due to particle pairs colliding with relative velocity less than $|w|$. While particles with a velocity larger than u_K are very few, they are responsible for a sizeable fraction of the collision rate. The data shown correspond to $\rho_p/\rho_f = 1000$. The ratio $u_K\tau_K/(2a) \approx 13.5$ at $St = 0.3$, panel (a), and ≈ 8.6 at $St = 0.75$, panel (b).

participating in a collision with a relative velocity w is proportional to the distribution of pairs, $P(w|2a)$, multiplied by $|w|$ (Wang *et al.* 2000), we deduced that $P(w|2a) \propto P_{coll}(w)/|w|$. Figure 5 shows the cumulative p.d.f., $C(|w|)$, and the contribution of particles of velocity $w' < |w|$ to the flux (Sundaram & Collins 1997), $C_\Phi(|w|)$:

$$C(|w|) = \int_0^{|w|} P(w'|2a)\,\mathrm{d}w', \tag{3.1}$$

$$C_\Phi(|w|) = \frac{\displaystyle\int_0^{|w|} P(w'|2a)w'\,\mathrm{d}w'}{\displaystyle\int_0^\infty P(w'|2a)w'\,\mathrm{d}w'}. \tag{3.2}$$

For the value of the Stokes number $St = 0.3$, at which figure 2 indicates that preferential concentration plays a very significant role in the collision rate, we find that particles with a relative velocity less than that of 99 % of all colliding particles have a relative velocity $|w| \leqslant 2(2a)/\tau_K$, and contribute to $\lesssim 85$ % of the total collision rate. On the other hand, at $St = 0.75$, for which figure 2 suggests a much more significant contribution of the sling effect, we find that approximately 99 % of all colliding particle pairs have a velocity $\lesssim 7(2a)/\tau_K$. These colliding particles however contribute only ~ 72 % of the total collision rate. In other words, 1 % of all pairs of particles have a very large relative velocity, of the order of the velocity u_K, but contribute to a significant fraction, of the order of 30 %, of the total collision rate. At yet higher values of St, the fraction of colliding particle pairs with relative velocities larger than u_K increases, and provides an ever larger contribution to the collision rate. The qualitative consistency between the results shown in figure 4 (obtained by using (2.6) and (2.8)), and those obtained by identifying the particle pairs colliding with

a large relative velocity, provides an independent justification of our approach, and suggests a possible alternative definition of the collision rate R_{sling}.

4. Discussion

An alternative decomposition of the collision rate, originally proposed by Sundaram & Collins (1997), expresses the collision rate R as a product in which the term $g(2a)$, which describes the local concentration enhancement around a particle, appears as an overall factor:

$$R = 2\pi(2a)^2 g(2a) \langle |w| \rangle_{eff}. \tag{4.1}$$

This representation, which is exact for a suitable definition of $\langle |w| \rangle_{eff}$, suggests that the preferential concentration and sling effects act together to enhance the collision rate. Numerical work (Sundaram & Collins 1996; Bec *et al.* 2010; Rosa *et al.* 2013) has provided detailed information on the two unknown terms in (4.1). While modelling work has provided an effective description of g and $\langle |w| \rangle$ (Zaichik *et al.* 2003), the results presented in this work indicate that, although logically consistent, the product representation (4.1) is not the most physically transparent approach. In particular, figure 1(*b*) demonstrates that, if this parametrisation of the collision rate is used, then the dependence of $g(2a)$ upon ρ_p/ρ_f shown in figure 3 must be cancelled (for $St \geqslant 0.5$) by a reciprocal dependence of the collision velocity, $\langle |w| \rangle_{eff}$. In fact, previous measurements (Bec *et al.* 2010; Rosa *et al.* 2013) of the dependence of $g(r)$ and of the average velocity difference as a function of r suggest power-law dependences, the exponents being such that the product $g(2a)\langle |w| \rangle_{eff}$ is essentially constant for $St \gtrsim 0.5$. Equations (2.6), (2.7) and (2.8) give a physically well-motivated theory, which explains the data, and provide an explanation for this cancellation. We remark that the power-law dependence of the collision velocity found in Gustavsson & Mehlig (2011, 2014), namely $\langle |w| \rangle_{eff} \propto (2a)^{3-D_2}$, effectively explains the observation that the product $g(2a)\langle |w| \rangle_{eff}$ is independent of $(2a)$, thus justifying (2.8) for that system.

We conclude that, in turbulent flows and at values of $\rho_p/\rho_f \approx 1000$ (the case relevant to typical aerosols), the sling effect provides at least 50 % of the collision-rate enhancement for $St \approx 1$, and prevails at higher values of the Stokes number, for $St \gtrsim 2$.

REFERENCES

ABRAHAMSON, J. 1975 Collision rates of small particles in a vigorously turbulent fluid. *Chem. Engng Sci.* **30**, 1371–1379.

BEC, J. 2003 Fractal clustering of inertial particles in random flows. *Phys. Fluids* **15**, L81–L84.

BEC, J., BIFERALE, L., CENCINI, M., LANOTTE, A., MUSACCHIO, S. & TOSCHI, F. 2007 Heavy particle concentration in turbulence at dissipative and inertial scales. *Phys. Rev. Lett.* **98**, 084502.

BEC, J., BIFERALE, L., CENCINI, M., LANOTTE, A. S. & TOSCHI, F. 2010 Intermittency in the velocity distribution of heavy particles in turbulence. *J. Fluid Mech.* **646**, 527–536.

BEWLEY, G. P., SAW, E.-W. & BODENSCHATZ, E. 2013 Observation of the sling effect. *New J. Phys.* **15**, 083051.

CHUN, J., KOCH, D. L., RANI, S. L., AHLUWALI, A. & COLLINS, L. R. 2005 Clustering of aerosol particles in isotropic turbulence. *J. Fluid Mech.* **539**, 219–251.

DAITCHE, A. & TÉL, T. 2011 Memory effects are relevant for chaotic advection of inertial particles. *Phys. Rev. Lett.* **107**, 244501.

DUCASSE, L. & PUMIR, A. 2009 Inertial particle collisions in turbulent synthetic flows: quantifying the sling effect. *Phys. Rev.* E **80**, 066312.

ELGHOBASHI, S. 1994 On predicting particle-laden turbulent flows. *Appl. Sci. Res.* **52**, 309–329.

FALKOVICH, G., FOUXON, A. & STEPANOV, M. G. 2002 Acceleration of rain initiation by cloud turbulence. *Nature* **419**, 151–154.

FALKOVICH, G. & PUMIR, A. 2007 Sling effect in collisions of water droplets in turbulent clouds. *J. Atmos. Sci.* **64**, 4497–4505.

GATIGNOL, R. 1983 Faxen formulae for a rigid particle in an unsteady non-uniform Stokes flow. *J. Méc. Théor. Appl.* **1**, 143–160.

GIBERT, M., XU, H. T. & BODENSCHATZ, E. 2012 Where do small, weakly inertial particles go in a turbulent flow? *J. Fluid Mech.* **698**, 160–167.

GRABOWSKI, W. W. & VAILLANCOURT, P. 1999 Comments on 'Preferential concentration of cloud droplets by turbulence: effects on the early evolution of cumulus cloud droplet spectra'. *J. Atmos. Sci.* **56**, 1433–1436.

GRABOWSKI, W. W. & WANG, L.-P. 2013 Growth of cloud droplets in a turbulent environment. *Annu. Rev. Fluid Mech.* **45**, 293–324.

GRASSBERGER, P. & PROCACCIA, I. 1983 Measuring the strangeness of strange attractors. *Physica* D **9**, 189–208.

GUSTAVSSON, K. & MEHLIG, B. 2011 Distribution of relative velocities in turbulent aerosols. *Phys. Rev.* E **84**, 045304.

GUSTAVSSON, K. & MEHLIG, B. 2014 Relative velocities of inertial particles in turbulent aerosols. *J. Turbulence* **15** (1), 34–69 (doi:10.1080/14685248.2013.875188).

IJZERMANS, R. H. A., MENEGUZ, E. & REEKS, M. W. 2010 Segregation of particles in incompressible random flows: singularities, intermittency and random uncorrelated motion. *J. Fluid Mech.* **653**, 99–136.

LAMORGESE, A. G., CAUGHEY, D. A. & POPE, S. B. 2005 Direct numerical simulation of homogeneous turbulence with hyperviscosity. *Phys. Fluids* **17**, 015106.

MAXEY, M. R. 1987 The gravitational settling of aerosol particles in homogeneous turbulence and random flow fields. *J. Fluid Mech.* **174**, 441–465.

MAXEY, M. R. & RILEY, J. J. 1983 Equation of motion for a small rigid sphere in a nonuniform flow. *Phys. Fluids* **26**, 883–889.

MEHLIG, B., USKI, V. & WILKINSON, M. 2007 Colliding particles in highly turbulent flows. *Phys. Fluids* **19**, 098107.

MENEGUZ, E. & REEKS, M. W. 2011 Statistical properties of particle segregation in homogeneous isotropic turbulence. *J. Fluid Mech.* **686**, 338–351.

PRESS, W. H., TEUKOLSKY, S. A., VETTERLING, W. T. & FLANNERY, B. P. 2007 *Numerical Recipes: The Art of Scientific Computing*. 3rd edn. Cambridge University Press.

READE, W. C. & COLLINS, L. R. 2000 Effect of preferential concentration on turbulent collision rates. *Phys. Fluids* **12**, 2530–2540.

ROSA, B., PARISHANI, H., AYALA, O., GRABOWSKI, W. W. & WANG, L.-P. 2013 Kinematic and dynamic collision statistics of cloud droplets from high-resolution simulations. *New J. Phys.* **15**, 045032.

SAFFMAN, P. G. & TURNER, J. S. 1956 On the collision of drops in turbulent clouds. *J. Fluid Mech.* **1**, 16–30.

SAFRANOV, V. S. 1969 *Evolution of the Protoplanetary Cloud and Formation of the Earth and the Planets*. Nauka. NASA Tech. Transl. F-677. NASA.

SALAZAR, P. L. C. & COLLINS, L. R. 2012 Inertial particle relative velocity statistics in homogeneous isotropic turbulence. *J. Fluid Mech.* **696**, 45–66.

SHAW, R. A. 2003 Particle–turbulence interactions in atmospheric clouds. *Annu. Rev. Fluid Mech.* **35**, 183–227.

SOMMERER, J. C. & OTT, E. 1993 Particles floating on a moving fluid: a dynamically comprehensible physical fractal. *Science* **259**, 335–339.

SUNDARAM, S. & COLLINS, L. R. 1996 Numerical considerations in simulating a turbulent suspension of finite-volume particles. *J. Comput. Phys.* **124**, 337–350.

SUNDARAM, S. & COLLINS, L. R. 1997 Collision statistics in an isotropic particle-laden turbulent suspension. Part 1. Direct numerical simulations. *J. Fluid Mech.* **335**, 75–109.

VÖLK, H. J., JONES, F. C., MORFILL, G. E. & RÖSER, S. 1980 Collisions between grains in a turbulent gas. *Astron. Astrophys.* **85**, 316–325.

VOßKUHLE, M., LÉVÊQUE, E., WILKINSON, M. & PUMIR, A. 2013 Multiple collisions in turbulent flows. *Phys. Rev.* E **88**, 063008.

WANG, L.-P., WEXLER, A. S. & ZHOU, Y. 2000 Statistical mechanical description and modelling of turbulent collision of inertial particles. *J. Fluid Mech.* **415**, 117–153.

WILKINSON, M. & MEHLIG, B. 2005 Caustics in turbulent aerosols. *Europhys. Lett.* **71**, 186–192.

WILKINSON, M., MEHLIG, B. & BEZUGLYY, V. 2006 Caustic activation of rain showers. *Phys. Rev. Lett.* **97**, 048501.

WILKINSON, M., MEHLIG, B., ÖSTLUND, S. & DUNCAN, K. P. 2007 Unmixing in random flows. *Phys. Fluids* **19**, 113303.

WILKINSON, M., MEHLIG, B. & USKI, V. 2008 Stokes trapping and planet formation. *Astrophys. J. Suppl.* **176**, 484–496.

ZAICHIK, L. I., SIMONIN, O. & ALIPCHENKOV, V. M. 2003 Two statistical models for predicting collisions rates of inertial particles in homogeneous isotropic turbulence. *Phys. Fluids* **15**, 2995–3005.